The Astrophysical Journal, 687:1448–1459, 2008 November 10

THE NATURE OF *p*-MODES AND GRANULATION IN PROCYON: NEW *MOST*[1] PHOTOMETRY AND NEW YALE CONVECTION MODELS

D. B. Guenther
Institute for Computational Astrophysics, Department of Astronomy and Physics, Saint Mary's University, Halifax, NS B3H 3C3, Canada

T. Kallinger, M. Gruberbauer, D. Huber, W. W. Weiss, R. Kuschnig
Institut für Astronomie, Universität Wien Türkenschanzstrasse 17, A-1180 Wien, Austria

P. Demarque, F. Robinson
Department of Astronomy, Yale University, New Haven CT 06511

J. M. Matthews
Department of Physics and Astronomy, University of British Columbia, 6224 Agricultural Road, Vancouver, BC V6T 1Z1, Canada

A. F. J. Moffat
Observatoire Astronomque du Mont Mégantic, Départment de Physique, Université de Montréal C. P. 6128, Succursale: Centre-Ville, Montréal, QC H3C 3J7, Canada

S. M. Rucinski
Department of Astronomy and Astrophysics, University of Toronto, ON M5S 3H4, Canada

D. Sasselov
Harvard-Smithsonian Center for Astrophysics, 60 Garden Street, Cambridge, MA 102138

and

G. A. H. Walker
Department of Physics and Astronomy, University of British Columbia, 6224 Agricultural Road, Vancouver, BC V6T 1Z1, Canada
Received 2008 February 12; accepted 2008 June 30

ABSTRACT

We present new photometry of Procyon, obtained by *MOST* during a 38 day run in 2007, and frequency analyses of those data. The long time coverage and low point-to-point scatter of the light curve yield an average noise amplitude of about 1.5–2.0 ppm in the frequency range 500–1500 μHz. This is half the noise level obtained from each of the previous two Procyon campaigns by *MOST* in 2004 and 2005. The 2007 *MOST* amplitude spectrum shows some evidence for *p*-mode signal: excess power centered near 1000 μHz and an autocorrelation signal near 55 μHz (suggestive of a mode spacing around that frequency), both consistent with *p*-mode model predictions. However, we do not see regularly spaced frequencies aligned in common *l*-valued ridges in echelle diagrams of the most significant peaks in the spectrum unless we select modes from the spectrum using a priori assumptions. The most significant peaks in the spectrum are scattered by more than ± 5 μHz about the predicted *l*-valued ridges, a value that is consistent with the scatter among individually identified frequencies obtained from ground-based radial velocity (RV) observations. We argue that the observed scatter is intrinsic to the star, due to short lifetimes of the modes and the dynamic structure of Procyon's thin convection zone. We compare the *MOST* Procyon amplitude and power density spectra with preliminary results of three-dimensional numerical models of convection by the Yale group. These models show that, unlike in the Sun, Procyon's granulation signal in luminosity has a peak coinciding with the expected frequency region for *p*-modes near 1000 μHz.

Subject headings: convection — stars: individual (Procyon) — stars: interiors — stars: oscillations

1. INTRODUCTION

Procyon A was the first primary science target star for the *MOST* (*Microvariability and Oscillations of Stars*) space telescope (Walker et al. 2003). *MOST*, launched in late 2003 June, observed Procyon in 2004 January for 35 days (Matthews et al. 2004), returning again the next year to confirm the previous year's results with 16 days of observations (Guenther et al. 2007). In 2007 January–February, to overlap with an independently planned ground-based spectroscopic campaign (Hekker et al. 2007), *MOST* re-observed Procyon for 38 days.

Initially, Procyon was chosen by the *MOST* science team as a high-priority target for the mission because of evidence for solar-type pulsation in ground-based spectroscopy (for example, Brown et al. 1991; Martic et al. 1999) and tight constraints offered by theoretical models (for example, Chaboyer et al. 1999). For a recent review see Chaplin et al. (2008). Based on both the available radial velocity (RV) observations and scaling arguments, we expected the luminosity oscillations in Procyon to be well above the few-ppm signal-to-noise threshold of the *MOST* instrument for this target.

Following the 2004 observations, Matthews et al. (2004; hereafter Ma2004) reported that they could not see any evidence for *p*-modes in the *MOST* photometry of Procyon. They concluded that, if there are *p*-modes on Procyon, the peak amplitudes have to be (conservatively) less than 15 ppm in luminosity and/or the mode lifetimes have to be shorter than 2–3 days. Modes with short lifetimes would yield multiple peaks in the

[1] Based on data from the *MOST* satellite, a Canadian Space Agency mission, jointly operated by Dynacon, Inc., the University of Toronto Institute of Aerospace Studies, and the University of British Columbia, with the assistance of the University of Vienna.

Fourier oscillation spectrum and thus would inhibit the identification of evenly spaced *p*-mode peaks. In addition, Ma2004 noted that, on first consideration, their results appeared to be at odds with theoretical expectations (Christensen-Dalsgaard & Frandsen 1983; Houdek et al. 1999) and in direct contrast with results from ground-based spectroscopy, based on RV-luminosity amplitude scaling relations widely accepted at that time. Bedding et al. (2005) responded by noting that, at the time, there already existed evidence that the amplitudes predicted by theoretical models were at least a factor of 2 larger than observed (Kjeldsen & Bedding 1995) for F-type stars similar to Procyon.

Régulo & Cortés (2005) and Marchenko (2008) re-analyzed the Ma2004 data and claimed to find evidence for *p*-mode oscillations, although they are careful to note that the results are tentative. Note that Régulo & Cortés (2005) identified spacings that in fact correspond to orbital artifacts in the 2004 *MOST* photometry. Baudin et al. (2008) performed time-frequency analyses of the 2004 data and confirmed the conclusions of Ma2004.

Bruntt et al. (2005) reported evidence for excess power around 1000 μHz in their two sets of photometry of Procyon with the star tracker on the *WIRE* (*Wide-field Infrared Explorer*) satellite, consistent with where *p*-mode power was reported in RV campaigns. They also noted a rising noise level at frequencies below 3000 μHz, which they interpreted as the granulation signal. However, the quality of the *WIRE* Procyon photometry is not sufficient to measure a large frequency separation for *p*-modes or to detect a comblike structure. Bruntt et al. (2005) argued that their findings, in contrast to the Ma2004 null result, suggest that *MOST* was suffering from unrecognized instrumental noise. We make direct comparisons of the *WIRE* and *MOST* photometry in this paper to refute that assertion.

Moving to the theoretical side, the Yale convection modeling group (Robinson et al. 2005) computed numerical hydrodynamical models of Procyon's thin convection zone for us, spurred in part by the controversy over the nature of *p*-modes in this star. Their models show that the superadiabatic peak (where *p*-modes are maximally driven by stochastic excitation) moves up and down, into and out of the optically thin region near the surface. This led us to wonder if there is a connection between Procyon's thin convection zone, the oscillating superadiabatic layer, and the lifetimes of the modes.

A recent thorough analysis of the uncertainties associated with the current state of the art in the construction of evolved stellar models of Procyon can be found in Provost et al. (2006). We note that the results of our own modeling of Procyon using the Yale Stellar Evolution code (Guenther et al. 2007) are consistent with their results. Provost et al. (2006) show that current observational data on Procyon, including asteroseismic data, are not yet stringent enough to constrain the models. In particular they point out that the large dispersion in reported *p*-mode large frequency spacing $\Delta\nu$ prevents the use of asteroseismology to constrain the models meaningfully.

The large spacing depends sensitively on the radius of the star and to a lesser extent on the internal structure. The radius of Procyon is not directly observable and is inferred from the star's known luminosity and surface temperature. The internal structure is derived from models constrained by the star's composition, mass, luminosity, and surface temperature. We draw attention to this because a new and distinct mass determination has appeared in the literature, which will have a small effect on the predicted large spacing.

The astrometric mass of Procyon, a binary system with white dwarf companion, was once thought to be $1.751 \pm 0.051\ M_\odot$ (Irwin et al. 1992). Stellar models of that era, based on the observed values of composition, luminosity, and effective temperature yielded significantly lower values, around $1.5\ M_\odot$ (Guenther & Demarque 1993; Chaboyer et al. 1999). Using improved orbital elements, Girard et al. (1996, 2000) recomputed the asteroseismic mass to obtain the modern value of $1.497 \pm 0.037\ M_\odot$ (based on the Hipparcos parallax $\pi = 0.2832'' \pm 0.0015''$), thereby removing the discrepancy between theory and observation. More recently, Schaefer et al. (2006) recomputed the orbit for Procyon and used the current revised Hipparcos parallax ($\pi = 0.28593'' \pm 0.00088''$) to recover a mass of $1.497 \pm 0.037\ M_\odot$. Although this value is identical to Girard's value, the orbit and the parallax used by Schaefer et al. are slightly different. The derived mass does depend on the assumed parallax. T. M. Girard (2008, private communication) computed the mass of Procyon using $\pi = 0.2832'' \pm 0.0015''$ and Schaefer et al.'s latest orbit, obtaining $1.5461 \pm 0.0472\ M_\odot$. Then, using the van Leeuwen value of $0.28452'' \pm 0.00127''$, he obtained $1.520\ M_\odot$. What is important to note here is that all these values are not far from the model value of $\sim 1.5\ M_\odot$.

Interestingly, however, lower values of Procyon's mass have surfaced in the literature, such as the Gatewood & Han (2006) estimate of $1.43 \pm 0.034\ M_\odot$ (see also Allende Prieto et al. 2002), also using the Hipparcos parallax. Although the lower values are within the observational uncertainty of the Girard et al. value, they are too low to be easily reconciled with stellar models since models with mass this low have lower luminosities than observed. Furthermore, it is not clear why there exists such a large discrepancy in the astrometric mass determinations of Procyon. The effect of the mass uncertainty on the *p*-mode large spacing in models is ~ 1 μHz.

In this paper, we present and discuss the *MOST* 2007 observations of Procyon. They are longer in duration and of higher quality than the previous two *MOST* runs. We compare our latest observations to the previous runs and to published RV observations obtained from the ground. We present and compare the results of our frequency analysis pipeline to results obtained using other reduction strategies. Our analysis is based on the well-tested SigSpec strategy developed by Reegen (2007), which assigns a probability of chance existence to each peak obtained in a discrete Fourier transform of a time series. We discuss alternative analysis strategies that assume prior knowledge about the modes, such as a regular spacing or short mode lifetimes. With regard to the latter, we model the effects of short lifetimes on synthetic oscillation spectra to show how they compare to our observations of Procyon's spectrum. Finally, we present some initial results of numerical simulations of Procyon's convection zone and show that these simulations raise new issues about the interpretation of *p*-mode and granulation observations of Procyon.

2. OBSERVATIONS AND DATA REDUCTION

The *MOST* space telescope is in a Sun-synchronous polar orbit, from which it is capable of obtaining precise uninterrupted photometry of bright stars in its continuous viewing zone for up to 2 months. The satellite is equipped with a 15 cm Maksutov telescope feeding a CCD through a custom broadband filter (350–700 nm). In its primary observing mode, a Fabry microlens projects an extended fixed image of the telescope pupil onto the CCD. Because the pupil image remains stable despite small pointing errors of up to $10''$,[2] this observing mode provides the most precise photometry obtainable.

[2] Note that *MOST* is a microsatellite with very low inertia, so such pointing accuracy had never been achieved for such a payload before *MOST*. *MOST* pointing accuracy is typically $\pm 1''$, about 4000 times better than ever achieved with earlier microsats.

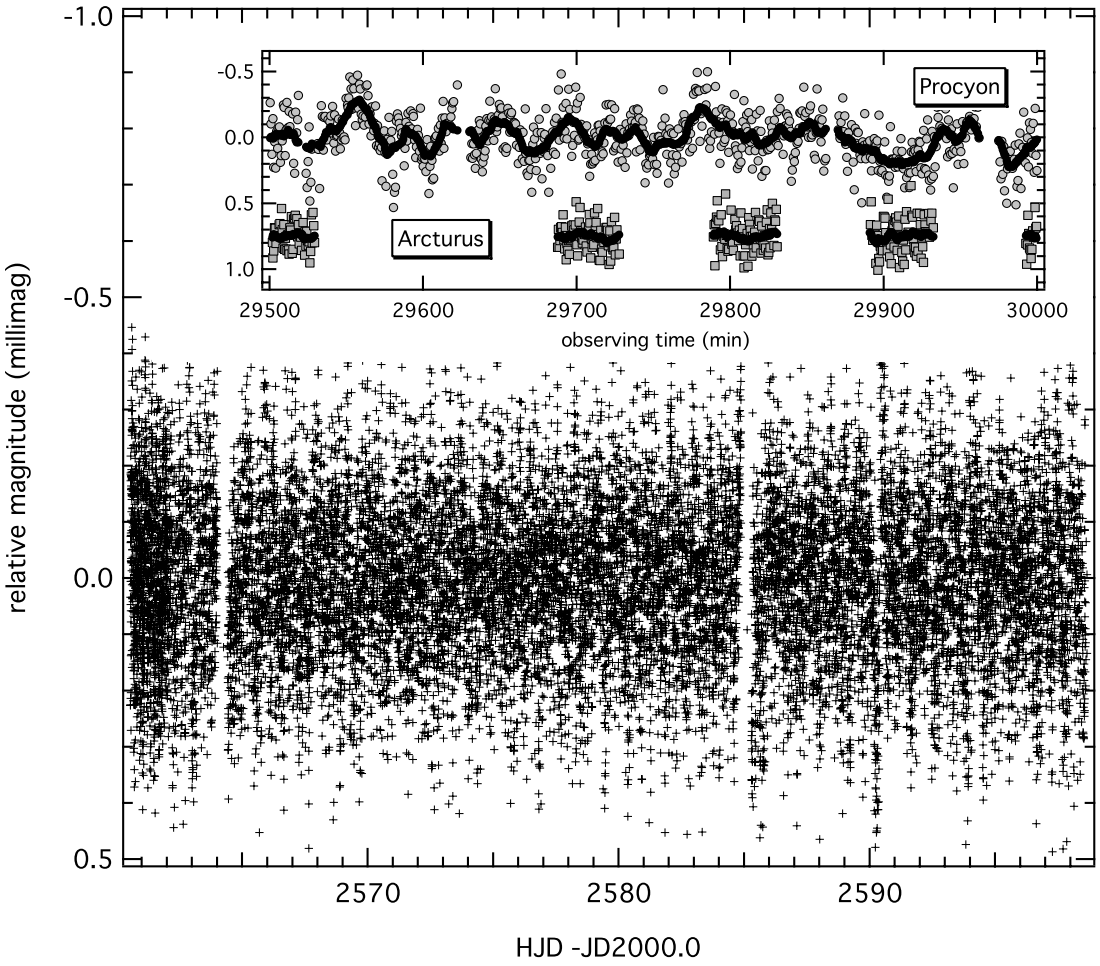

FIG. 1.—Detrended and binned light curve of the *MOST* 2007 Procyon run. The plus symbols are averages of five consecutive data points (so each binned point covers about 3 minutes). The inset shows an expanded view of about 8 hr of the unbinned data (*filled circles*) with a running average (*solid curve*), compared to the *MOST* 2007 light curve of Arcturus (*filled squares*) on the same scale (but shifted in time). The Arcturus photometry was collected in the same way as the Procyon photometry but not at the same time.

During the first 2 yr of the *MOST* mission, an additional CCD detector was used for star tracking. This detector stopped working in early 2006 when its support electronics suffered a particularly energetic particle hit. Star tracking was then relocated to the open field section of the CCD originally dedicated solely to science measurements. Because the satellite's attitude control system requires guide star positions to be read out once every 1–3.5 s, science field exposures are now stacked onboard to achieve the desired signal-to-noise ratio (S/N) for each measurement. Although this adapted observing mode complicates the data reduction process, it does provide higher total count rates per exposure and therefore better S/N than in the original observing mode. Due to upgrades in attitude control software and operation, *MOST* pointing during the 2007 Procyon run was significantly better than it was during the 2004 Procyon observations.

Procyon was observed as a Fabry imaging target during 2007 January 3–February 11. A total of 96,195 exposure stacks were made, with each exposure stack containing 31 subexposures, yielding a stacked exposure time of about 24.8 s at a sampling interval of 37 s. The standard reduction pipeline for *MOST* Fabry imaging targets, described in Reegen et al. (2006), was used. This reduction is primarily designed to remove stray light effects in the data caused by earthshine scattered into the focal plane and modulated by periodicities in the *MOST* satellite orbit.

The reduction code is mainly based on calculating and removing the correlations between pixels illuminated by starlight (hereafter "target pixels") and sky background (hereafter "background pixels") over time. First the relation between mean target and mean background intensity is computed and corrected by subtracting a linear fit to the correlation. Then the image is corrected using the background pixel showing the best correlation coefficient with the residual mean target intensity. This reduction step is performed iteratively. Due to the fact that stray light is variable over smaller timescales than the length of a typical *MOST* run, these decorrelations are performed on small subsets of typically five *MOST* orbits (5×101 minutes ~ 0.3 days) rather than for the observing run as a whole.

In the original applications of this decorrelation technique, a fixed list of correlation coefficients for background pixels was calculated once for each reduction subset treated. We realized, however, that in the new observing mode with image stacking, this strategy was not the most efficient method to remove stray light. To improve the reduction process, we incorporated an additional correlation computation after each iteration, rather than just once for each subset. The refined decorrelation procedure suppresses the instrumental frequencies more effectively and in fewer iteration steps. For the Procyon 2007 data, the total number of iterations was adopted to be 50, yielding a reduction of the average amplitudes of orbital modulation of stray light from (typically) 1500 ppm to about 20 ppm.

Figure 1 shows the final reduced light curve (binned for better visibility) of the *MOST* Procyon 2007 run with all power at

TABLE 1
MOST Procyon Observation Statistics

Year	Duration (days)	Point-to-point Scatter (ppm)	Time-domain rms (ppm)	Noise at 8–10 mHz (ppm)
2004.....	35.0	314	1245	2.25
2005.....	16.0	275	530	2.78
2007.....	38.5	140	196	0.88

frequencies less than 2 cycles day^{-1} removed. Beyond the stray light correction, the reduction pipeline identifies and removes CCD frames with Fabry image geometry indicating star misalignment with the microlens field stop, or an excessive number of cosmic ray impacts (see Reegen et al. [2006] for details). This leaves a reduced light curve with an effective duty cycle of ~81%. The inset of Figure 1 is a close-up of the unbinned light curve, revealing light variations on timescales as short as a few minutes, close to what is expected for solar-like oscillations in this star.

To test that any variations seen in Figure 1 are not due to instrumental noise or systematic drifts, we compare the Procyon 2007 data set to the light curve of Arcturus also obtained by *MOST* in 2007. The light curve of the somewhat brighter star Arcturus ($V = -0.04$ mag, compared to $V = +0.35$ for Procyon) has a slightly lower point-to-point scatter of ~130 ppm (compared to 140 ppm in the Procyon data) but does not show light variations on timescales of minutes. It is very unlikely that the obvious variations in Procyon are of instrumental origin. (Note that Arcturus was not observed continuously during each 101 minute *MOST* orbit, which accounts for the periodic gaps in the light curve shown in the inset of Fig. 1.) The reduced Procyon 2007 light curve and the raw data files are available in the *MOST* Public Data Archive.[3]

3. FREQUENCY ANALYSIS

Procyon was the first primary science target observed by *MOST* following the commissioning phase of the mission. The data collected in early 2004 spanned 32 days and presented the most complete and precise light curve of Procyon to that date (Ma2004). Although a noise level in the Fourier domain of only about 3 ppm was reached, the analysis did not reveal any unambiguous detection of *p*-mode oscillations above that level. *MOST* returned to Procyon 1 yr later, gathering about 16 days of photometry with a duty cycle close to 100%. With better pointing stability and an improved data reduction pipeline (Guenther et al. 2007), the rms scatter of the light curve was 1/2 that of the 2004 run, but the shorter timespan of the observations resulted in a noise level in Fourier space that was comparable. Once again the frequency analyses did not yield any clear detection of pulsations in the star.

The 2007 *MOST* observation run of Procyon supersedes both the 2004 and 2005 runs. Even though the data were gathered 3 yr beyond the nominal mission lifetime, the 2007 Procyon data represented the most precise measurements of a star ever obtained by *MOST*, exceeding the quality of both the 2004 and 2005 Procyon photometry. Table 1 compares the observational statistics of all three *MOST* runs of Procyon. Figure 2 compares the smoothed Fourier amplitude spectra of the three time series, calculated for bins of 10 cycles day^{-1} (~116 μHz). The 2007 run outperforms the earlier data sets with a noise level of ~0.9 ppm in the range 8–10 mHz, which is the same frequency range used by Bruntt et al. (2005) to define the noise level of *WIRE* photometry of Procyon. They measured the white noise levels in their 1999 and 2000 *WIRE* amplitude spectra in that frequency range to be 1.8–1.9 ppm. In the same range, their independent analysis of the *MOST* 2004 Procyon amplitude spectrum yielded a lower noise level of 1.6 ppm. Our measurement in Table 1 of the noise level of the 2004 *MOST* data is higher because our new stray light corrections remove more of the target pixels and result in somewhat larger Poisson noise. We compare and discuss the noise levels and characters of the *MOST* and *WIRE* photometry of Procyon in § 5.

We believe that the rise in power at low frequencies, below 0.35 mHz, is mostly due to residual instrumental and environmental drifts, and to lingering orbital modulation terms in the stray light close to the fundamental and first overtone of the *MOST* satellite orbital frequency (0.165 and 0.330 mHz). Other sources could include intrinsic stellar variability on long timescales. We note that owing to the clean spectral window we do not expect very much of the power in the low-frequency range to leak into the *p*-mode frequency range.

The *MOST* 2007 light curve has point-to-point scatter of about 140 ppm. Taking the average photon flux level (4.78×10^8 ADU) and a gain of 6.1 e^- ADU^{-1}, the pure photon noise level is ~18 ppm, about 8 times less than the point-to-point scatter. Bruntt et al. (2005) suggested that the difference between the observed point-to-point scatter and the photon noise level in the *MOST* 2004 data (a factor of about 4) might be due to instrumental noise, based on a factor of 1.2 they determined for their own *WIRE* observations of Procyon. While the difference in the photon noise and point-to-point scatter for *MOST* 2007 data of Procyon might be partially due to instrumental noise, we doubt that this can entirely account for the non–white noise in the data since such a difference has not been recorded for other *MOST* targets. We discuss in § 5 the possibility that granulation signal in Procyon could explain some of the observed noise level in the *MOST* photometry above photon noise.

The *MOST* 2007 light curve of Procyon was frequency analyzed with SigSpec (Reegen 2007). Using traditional Fourier analysis techniques, SigSpec computes a quantity called "spectral significance," which uses both frequency and phase information to compute the false alarm probability that a given peak of

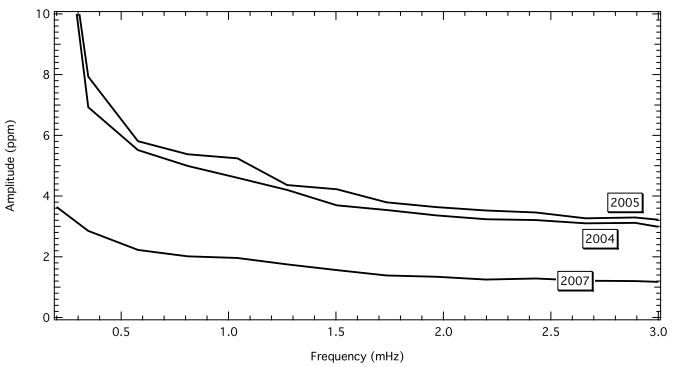

FIG. 2.—Smoothed Fourier amplitude as a function of frequency for all three *MOST* Procyon data sets.

[3] Accessible at http://www.astro.ubc.ca/MOST (on the "Science" page).

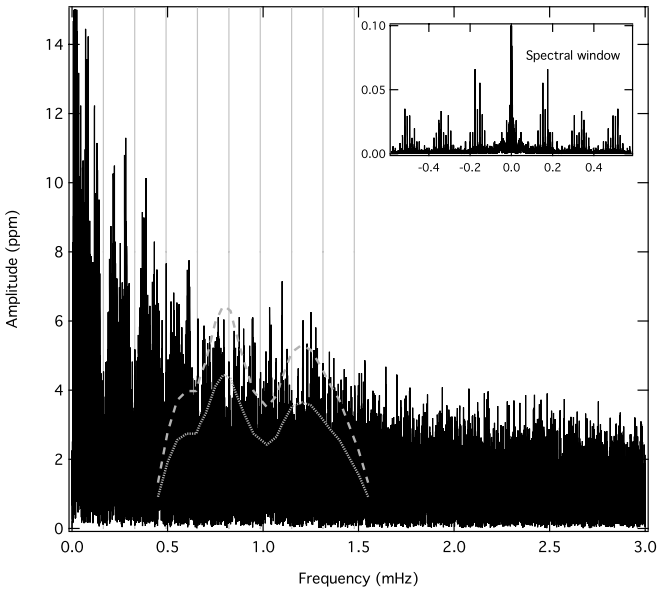

FIG. 3.—Fourier amplitude spectrum of the *MOST* 2007 Procyon data. Previously published average amplitudes transformed from rms RV variations reported by Leccia et al. (2007) are shown. The dotted gray line corresponds to the scaled peak Lorentzian profile height for the Leccia et al. results, and the dashed gray line corresponds to the scaled peak amplitude of the modes according to our simulations of modes with 2 day lifetimes (see Fig. 6). Vertical gray lines label *MOST*'s orbital frequency and its first several harmonics. The inset presents the spectral window of the *MOST* time series. (Note the truncated scale; the central peak of the window has a full amplitude of 1.0. The largest sidelobes, spaced by the orbital frequency of the *MOST* satellite, have amplitudes of only about 7% of the central peak).

given amplitude is caused by random white noise. The spectral significance (abbreviated sig) is logarithmic. A peak with sig = 5 is expected to be reproduced with the same amplitude, frequency, and phase by only 1 in 10^5 time series composed of white-noise spectra (Reegen 2007). Higher levels of spectral significance correspond to lower probabilities that the frequency peak can be attributed to white noise. We can therefore attribute a high sig peak as being either intrinsic to the star, instrumental, or non–white noise. Spectral significance can be transformed to the more traditional S/N estimate according to sig $\approx 0.341(\mathrm{S/N})^2$ (assuming only white noise).

Figure 3 presents the complete Fourier amplitude spectrum of the *MOST* 2007 Procyon photometry. Also shown are the amplitudes estimated from the RV measurements of Leccia et al. (2007, their Fig. 8), based on the RV-luminosity oscillation amplitude calibration of Kjeldsen & Bedding (1995), where we adopt $T_{\rm eff} = 6530$ K (Bedding et al. 2005) and set $\lambda = 525$ nm (the central wavelength of the *MOST* filter). The rms luminosity amplitude of Leccia scales according to $A^2 = HT/(4\tau)$, where A is the rms amplitude, T is the observing time, τ is the mode lifetime, and H is the Lorentzian profile height in the power spectrum. With $T = 38.5$ days and $\tau = 2$ days, the peak height of the Lorentzian profile in amplitude is 1/2.19 times the rms amplitude. This is shown in Figure 3 by the dotted line. The highest amplitude peak of the mode on average, according to our simulations (see Fig. 6), is about 1.45 times the height of the Lorentzian amplitude. This is shown in Figure 3 as the dashed line.

The "picket fence" of peaks expected for high-overtone solar-type acoustic modes is not readily apparent in our data. While we do observe some small power excess around 1000 μHz, the amplitudes reached are in most cases well below the values predicted from spectroscopic observations and the standard scaling relation. Only the frequencies most recently published by Leccia et al. (2007) have amplitudes comparable to the peaks in our spectrum.

4. INDIVIDUAL *p*-MODES IN THE *MOST* PHOTOMETRY?

Starting from the assumption that there are *p*-modes present in the *MOST* Procyon photometry, we identify individual frequencies in the amplitude spectrum which are possible *p*-mode candidates. However, given the low noise levels (and the lack of intrinsic signal frequencies in the star which rise well above the noise), we find that the specific peaks extracted depend on the algorithm used to identify them. Needless to say, the more model-dependent knowledge we build into the extraction process, the more the resultant frequencies reflect the model predictions.

There are a number of reasons to maintain a relatively unbiased approach to identifying *p*-modes in the spectrum of Procyon (and, of course, other stars). In addition to establishing the existence and nature of *p*-modes on Procyon, we want to use the *p*-modes to constrain stellar models and to test dynamical simulations of the surface layers, where Procyon's thin convection envelope presents a number of challenges to stellar modelers that have not yet been fully met. Consider, for example, that the timescale for the gravitational settling of helium out of Procyon's thin surface convection zone is so short that standard stellar evolutionary modeling predicts all of the helium (along with other heavier elements) should have been drained from the surface by the time the star reaches Procyon's current age. This prediction is clearly not borne out by observation. The modeling of the diffusion of helium is simply not sophisticated enough to take into account all the dynamical (and radiative) processes that are contributing to the flux of helium. With the aid of asteroseismic observations of Procyon, we should be able to calibrate the density distribution of helium in the outer layers as has been done successfully for the Sun.

There is also the possibility that the *p*-modes vary in amplitude at a level that is detectable and/or in frequency on timescales that are comparable to or less than the duration of the observations. We entertain this possibility again because (1) it was one possible explanation of the null detection of Procyon *p*-modes in *MOST* photometry compared to ground-based RV detections, and (2) hydrodynamical simulations (Robinson et al. 2005) of Procyon's convective envelope show that the average temperature structure itself is varying on timescales of minutes to hours, an effect that is not seen in the simulations of the Sun's convective envelope. An unbiased extraction of a reasonably complete set of *p*-modes could help prove or disprove the validity of this numerical result.

In order not to obscure possible new physical phenomena that may be revealed by the *MOST* photometry, we begin with our least biased extraction methodology, one that makes only a few assumptions about the nature of the nonintrinsic signal in the data, and makes no stellar-model-dependent assumptions.

4.1. *Standard Extraction*

To extract possible candidate *p*-mode frequencies, SigSpec was applied to the light curve. Using sequential prewhitening steps, all significant frequencies, i.e., frequencies with sig ≥ 4, below $\sim$4500 μHz were selected from the data. The same procedure was applied to a light curve constructed by averaging the intensities of all background pixels for each exposure. Then only frequencies unique to the target pixel data and not found in the background pixel data (within the frequency resolution of the data set) were considered. All frequencies corresponding to known

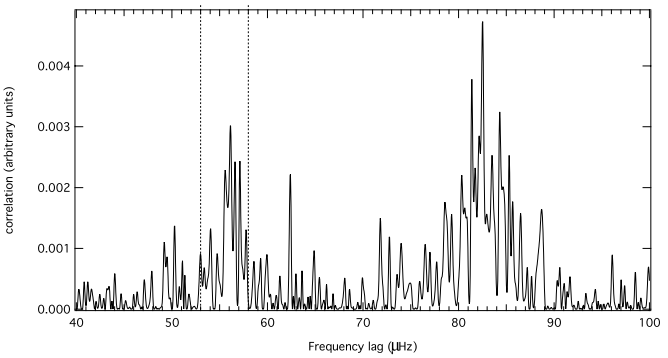

FIG. 4.—Autocorrelation of the DFT between 500 and 1500 μHz. The strongest peak corresponds to half of the *MOST* satellite's orbital frequency. The dashed lines indicate the range for the *p*-mode large frequency separation suggested by analyses of RV data in the literature.

instrumental artifacts such as the orbital frequency and its harmonics were automatically removed from consideration. Finally, from the remaining set of frequencies, only those with spectral significance greater than 5.46 (corresponding to an amplitude S/N ratio of about 4) were considered. The final list of *p*-mode candidates consists of 56 peaks in the frequency interval 500–1500 μHz (the expected range for *p*-modes in Procyon) with amplitudes ranging from 4.3 to 6.9 ppm.

To detect possible regular spacings of frequencies in our data set, we performed an autocorrelation of the DFT (discrete Fourier transform) power in the frequency range from 500 to 1500 μHz (Fig. 4). While the strongest correlation appears at half the satellite's orbital frequency ($\sim$82.1 μHz), the next best correlation, at $\sim$56 μHz, matches the range of large frequency spacings reported in some of the RV data (53–58 μHz).

The echelle diagram (Fig. 5) for the extracted peaks, constructed for a folding frequency of $\sim$56 μHz, does not show well-defined vertical ridges as predicted by standard stellar models of Procyon, although there is some hint of peaks concentrated along folded frequencies of $\sim$11 and $\sim$42 μHz. Furthermore, there are few coincident peaks among our observations and the ground-based results of Eggenberger et al. (2004) and Leccia et al. (2007). We exclude the Martic et al. (2004) results from this comparison since their published frequencies have been adjusted to include 1 cycle day^{-1} alias corrections that force nonaligning modes to fall along the expected ridges, opening another degree of freedom to tune an echelle diagram. At this stage we want to compare the dominant peak frequencies we find in the *MOST* photometry with the unaltered dominant peak frequencies found by others in other data sets.

With the *MOST* 2007 light curve of Procyon showing some evidence for oscillatory behavior above the noise which is not seen in a comparably bright target, Arcturus (see the inset of Fig. 1), it is surprising to us that there are so few coincidences among the observed photometric and RV frequencies. Indeed, the lack of agreement between any of the observations needs to be understood before selecting any one set of identified *p*-mode frequencies for model analysis. Finally, we note that quite a few of the frequencies fall well away from the central lines of any perceived ridges in the echelle diagram. This, we believe, may be an intrinsic characteristic of the *p*-mode frequencies on Procyon. We note that our 2007 Procyon run was timed to overlap with a ground-based effort involving several networked telescopes at different sites around the world resulting in a total of 472 spectroscopic hours (Hekker et al. 2007). A comparison of the results

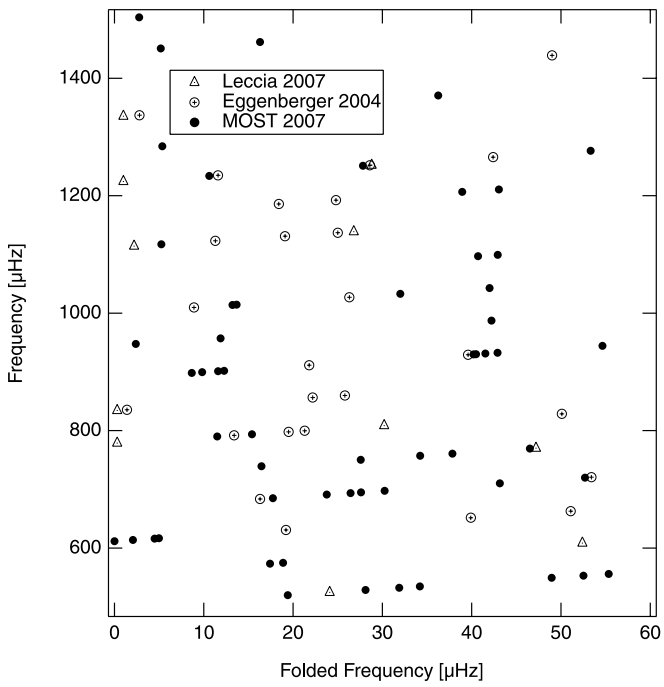

FIG. 5.—Echelle diagram with folding frequency 55.6 μHz showing the frequencies extracted from the *MOST* 2007 Procyon photometry using SigSpec in the range 500–1500 μHz. For comparison, frequencies reported by Leccia et al. (2007) and Eggenberger et al. (2004) in their RV campaigns are also shown.

of our *MOST* photometry and that spectroscopic campaign will be forthcoming.

The difficulties we have in extracting and uniquely identifying individual *p*-mode frequencies from the oscillation spectrum of Procyon could be because (1) the oscillation modes have relatively short lifetimes; and/or (2) the oscillation spectrum is largely the surface manifestation of convective motions. The first possibility is considered in the following subsection, and the second is the subject of § 5.

4.2. *Short Mode Lifetimes*

What if the lifetimes of the *p*-modes on Procyon are short enough (a few days or less) that, over the 5 week duration of the *MOST* observations, the amplitudes of individual modes rise and fall significantly? Instead of a single well-defined peak in the Fourier spectrum corresponding to the frequency of the oscillation, one will see multiple peaks distributed in an approximately Lorentzian profile surrounding the intrinsic oscillation frequency of the mode.

In Figure 6 we show the spectrum of a single frequency with a simulated 2 day lifetime sampled in time in the same way as the *MOST* 2007 Procyon run. The isolated frequency peak splits into a forest of peaks centered on the frequency that would be present if the oscillation had infinite lifetime. If all the observable modes in Procyon's spectrum have lifetimes on the order of days, then it is impossible to directly select the true peak frequencies from the superposed forest of peaks. We find in simulations that we can better extract the true mode peaks if we first smooth the spectrum by folding it with a Lorentzian profile of the appropriate lifetime.

To test this approach on the Procyon photometry, we build a set of frequencies following the asymptotic relation, applied amplitudes from the envelope suggested by Leccia et al. (2007), and simulated driving and damping to yield 2 day mode lifetimes using an approach described by Chaplin et al. (1997). We also

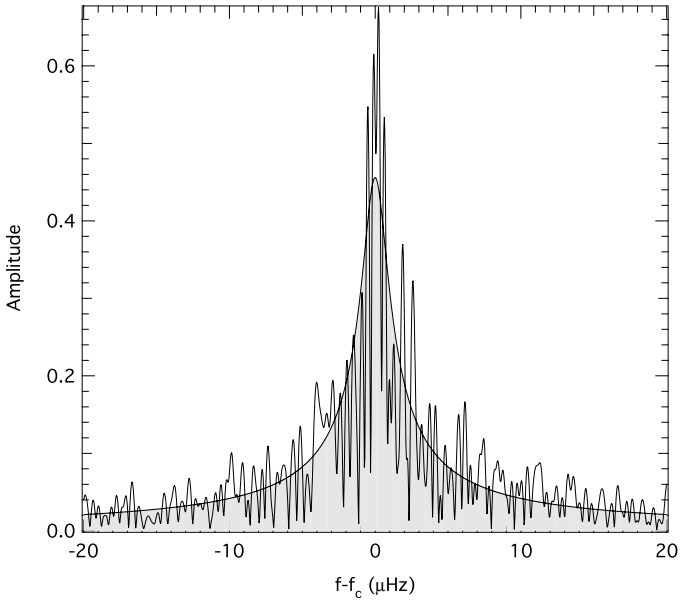

FIG. 6.—Simulation of how a damped and stochastically re-excited oscillation signal with a lifetime of 2 days would appear in the *MOST* 2007 Procyon data. The gray-shaded area indicates the corresponding Lorentzian profile. The original mode rms amplitude is 1.0. The height of the resultant Lorenztian profile is ~0.46, which is what one expects for an observing run of 38.5 days. The height of the highest peak is ~0.68 (i.e., 1.45 times the height of the Lorenztian profile).

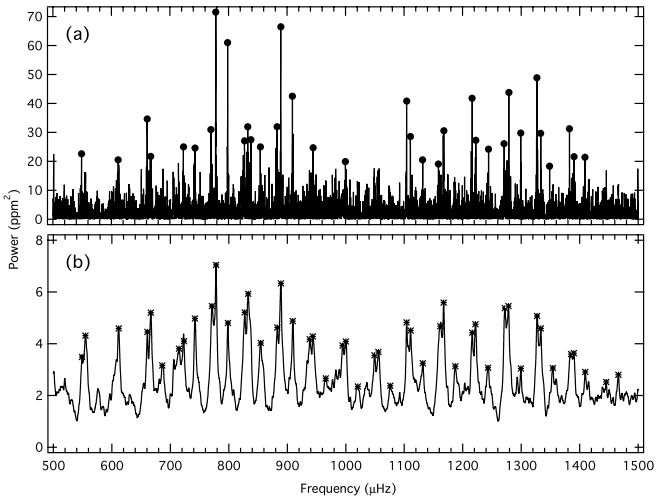

FIG. 7.—(*a*) Simulated *p*-mode spectrum with amplitudes based on the scaled envelope (see discussion for Fig. 3) provided by Leccia et al. (2007) and with noise added corresponding to the *MOST* 2007 run. The dominant peaks are indicated by filled circles. (*b*) Lorentzian-smoothed spectrum with the dominant peaks indicated by asterisks.

added noise to the spectrum at a level corresponding to the noise level in the *MOST* 2007 data. The resulting amplitude spectrum is shown in Figure 7*a*. A Lorentzian running average with a 2 day lifetime was then applied to the spectrum, yielding the smoothed spectrum shown in Figure 7*b*.

The frequency peaks from the original spectrum (Fig. 7*a*, *filled circles*) compared to the input frequencies (*open circles*) are shown in the echelle diagram of Figure 8*a*. The frequency recovery is marred by a large number of spurious frequencies that fall well away from the vertical ridges of the input frequencies. The frequency peaks from the Lorentzian smoothed spectrum (Fig. 7*b*, *asterisks*) compared to the input frequencies (*open circles*) are shown in Figure 8*b*. The number of spurious frequencies is considerably reduced, although not completely eliminated. If the *p*-modes in Procyon have short lifetimes of the order of several days and unless additional assumptions are made in selecting the peaks, the significant peaks selected from the Fourier spectrum of the *MOST* photometry will naturally include spurious frequencies.

Applying a 2 day Lorentzian running average to the *MOST* 2007 Procyon power spectrum yields the smoothed spectrum shown in the left panel of Figure 9. We take all well-detached peak frequencies (*dots in the left panel*) that exceed the average power (*dashed line*) and plot them in an echelle diagram with a folding frequency of 55.6 μHz. There is a much stronger indication of *p*-mode-like ridges in this version of the echelle diagram. However, the scatter of about ± 5 μHz from a well-defined ridge is still much greater than the observational uncertainties.

Although we conducted this test assuming a mode lifetime of 2 days, to match the known lifetimes of the modes we inserted in the simulation, the Lorentzian running average method is relatively insensitive to the assumed lifetime (i.e., Lorentzian width). We have tested the approach with running averages of lifetimes from 1 to 6 days and the result is still very successful in extracting the genuine input *p*-mode frequencies.

Our choice of the mode lifetime of 2 days in the simulations above is based on the character of the time-frequency analyses of the *MOST* 2007 Procyon photometry, like the plot shown in the top panel of Figure 10. In this analysis, the data are binned into 5 day–long subsets with each subset stepping forward in time every 0.25 days. The data in each subset is reduced as described in § 3. Figure 10 (*top*) clearly shows that significant peaks come and go over time.

We are able to simulate the behavior seen in the time-frequency plots of the *MOST* photometry by assuming the modes have short lifetimes. In the bottom two panels of Figure 10, we compare the amplitudes in simulated spectra of Procyon *p*-modes with 2 and 6 day mode lifetimes, sampled like the actual *MOST* 2007 data. We find that a lifetime of 2 days better mimics the observed time-frequency behavior.

Under the assumption that the modes do have short lifetimes, we developed the following method of peak frequency extraction. In the significance spectrum we look for recurring significant peaks in each 5 day subset (with 0.25 day steps), assuming that they come and go over the entire run, by noting all discrete frequency bins with sig > 6. To construct a combined spectrum, we then assign each frequency bin the highest significance found among the subsets. Subsequently, we select the highest peak and compute a frequency for it by averaging frequencies of the neighboring peaks within 1.10 μHz (approximately corresponding to the expected envelope of a Lorentzian profile due to a mode lifetime of 2 days). Since no prewhitening is performed, and in order to remove spurious signal and minimize the potential of misidentifying peaks produced by aliasing, all other significant frequency values closer than 17.36 μHz (=1.5 cycles day^{-1}) to the selected peak are removed from the spectrum. We then select the next highest peak, excluding the ± 17.36 μHz range defined by the first peak, and determine its frequency by averaging the frequencies within ± 1.10 μHz of it. The process is repeated until all peaks above sig $= 6$ are selected. We are aware that we might neglect some possibly intrinsic signal by excluding a certain range about a peak for further analysis. However, the computations in each iteration are based on the highest peak in the combined spectrum. Thus, we argue that this method produces an

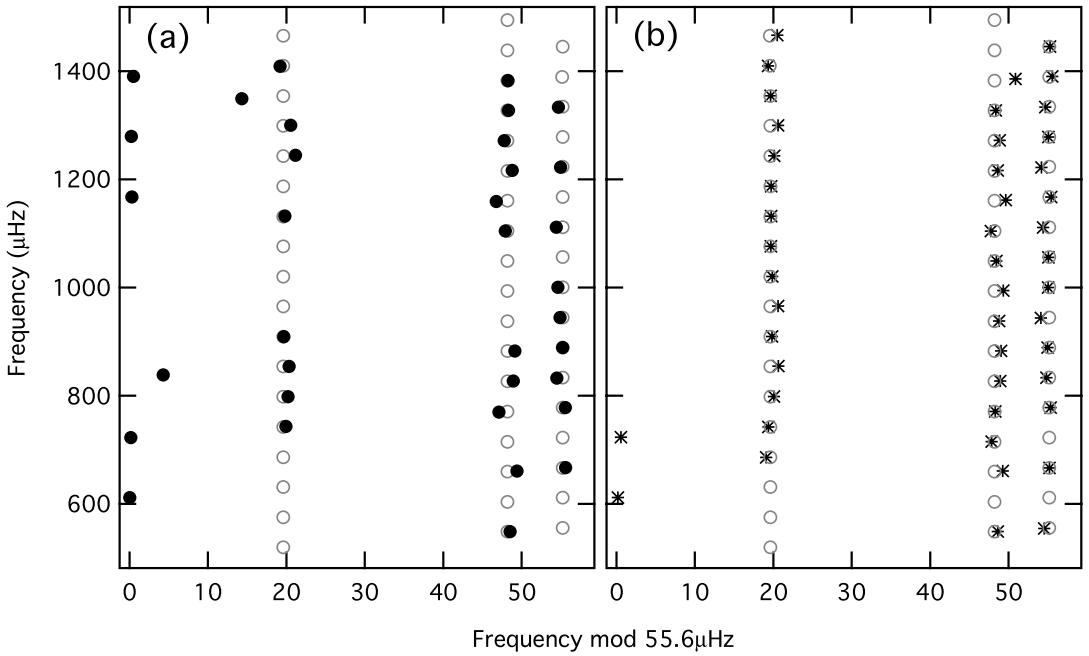

FIG. 8.—(*a*) Input frequencies for the simulated oscillation spectrum of Fig. 7*a* (*open circles*) are plotted with the peak frequencies which are recovered in that simulated oscillation spectrum (*filled circles*). (*b*) Same as (*a*) but the peak frequencies are selected from the Lorentzian-smoothed oscillation spectrum of Fig. 7*b*.

echelle diagram, without the problem of spurious signal, which is helpful to study the large frequency separation in an unbiased fashion. The resulting echelle diagram is shown in Figure 11. Within the inherent ± 2.3 μHz uncertainties, a ridge structure is clearly defined.

4.3. *Comb Filtering*

Comb filtering is an often-used technique to try to identify the *p*-mode frequencies in a noisy stellar oscillation spectrum. For detailed descriptions of the comb filtering technique, see Kjeldsen & Bedding (1995) or Leccia et al. (2007).

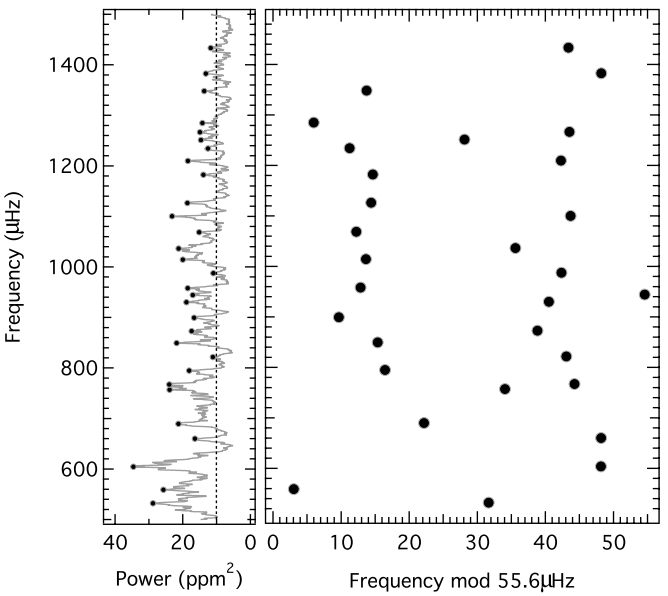

FIG. 9.—*Left*: 2 day Lorentzian running average of the *MOST* 2007 Procyon power spectrum in the frequency range where *p*-modes are expected. The dashed line indicates the average power level, and the dots are the frequencies we extract from this smoothed spectrum. *Right*: Echelle diagram of the extracted peak frequencies.

We consider the method to be too biased to provide a true extraction of the intrinsic pulsation behavior of the star. The assumed spacing for the comb filter, taken to be close to the value of the large spacing predicted by models and/or from autocorrelation of the power spectrum, does indeed select the best-looking peaks from the point of view of producing well-defined ridges in an echelle diagram. However, this approach completely ignores the significant peaks that are excluded, offering no explanation for their existence or justification for their removal.

Nevertheless, to compare the frequency content of the *MOST* 2007 Procyon photometry with analyses of other data sets in the literature, we have applied the comb filter technique to our data. Following the procedure described by Kjeldsen & Bedding (1995), we calculated the comb response in the frequency range 500–1500 μHz of our Procyon power spectrum for candidate values of the large frequency separation $\Delta\nu$ from 40 to 70 μHz. The results are shown in the top panel of Figure 12.

We then extract peak frequencies from the Procyon power spectrum following the regular pattern defined by the large frequency separation with the maximum comb response at 55.6 μHz (which is consistent with our autocorrelation result above). The identified frequencies are labeled by dots in the spectrum shown in the bottom left panel of Figure 12. The resulting echelle diagram (Fig. 12 *bottom right*), not surprisingly, shows strong ridge structure at the comb spacing. That echelle diagram is characteristic of $l = 0$, 1, and 2 *p*-modes and indeed can be well fitted by a stellar model of Procyon. But because the process of selecting mode frequencies inherently assumes that the modes follow a ridgelike structure with a characteristic spacing, the model fit is largely predetermined.

Comb filtering does not explain why other modes are excluded. To demonstrate the potential dangers of comb filtering, we applied the same technique to simulated granulation noise. The simulated light curve of granulation noise (effectively colored noise) was generated by taking the Procyon time sampling and adding 2000 sine functions with frequencies ranging from 0 to 200 cycles day^{-1} with 0.1 cycles day^{-1} steps. The amplitude of each sine function was obtained from a Gaussian random-number generator with the

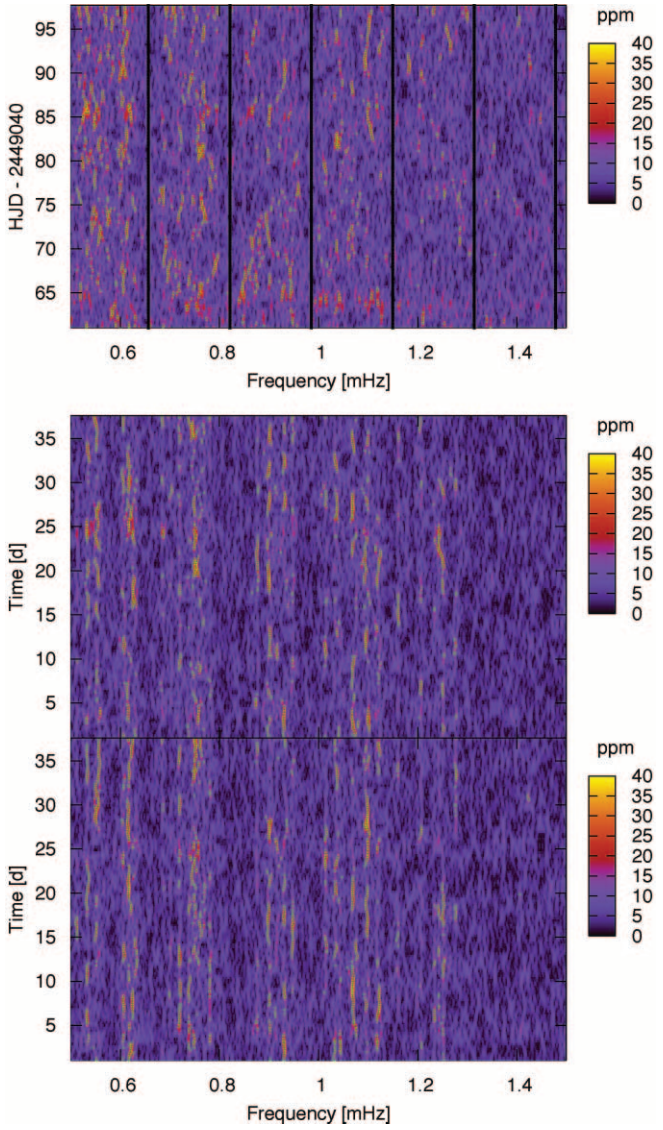

FIG. 10.—Time-frequency amplitude spectrum of the *MOST* 2007 Procyon photometry compared to two simulations: one with 2 day mode lifetimes, the other with 6 day lifetimes. The 2 day simulation appears to better mimic the main features of the observed Procyon time-frequency spectrum.

full width at half-maximum (FWHM) following an exponential decay with increasing frequency. The resulting power spectrum (Fig. 13) shows an artificially produced power excess around 600 μHz. We then applied the comb filter technique to the frequency range around this power excess and find a reasonable comb response at 78.7 μHz (Fig. 14, *top*). Based on this, we extracted peak frequencies as we did above for the real *MOST* data, and we find clear ridgelike structure in the echelle diagram (Fig. 14, *bottom*) even though the input light curve contains no *p*-modes or any actual stellar model physics.

5. GRANULATION

In parallel with *MOST* observations of Procyon, the Yale Convection Group has been computing three-dimensional numerical convection models to match the surface convection zone of Procyon. The convection modeling is described in Robinson et al. (2005) and Robinson & Demarque (2007); modeling results for the Sun are described in Robinson et al. (2003); comparisons of the convection modeling results for the Sun to other solar simulations is summarized in two reviews by Kupka (2005, 2008), in

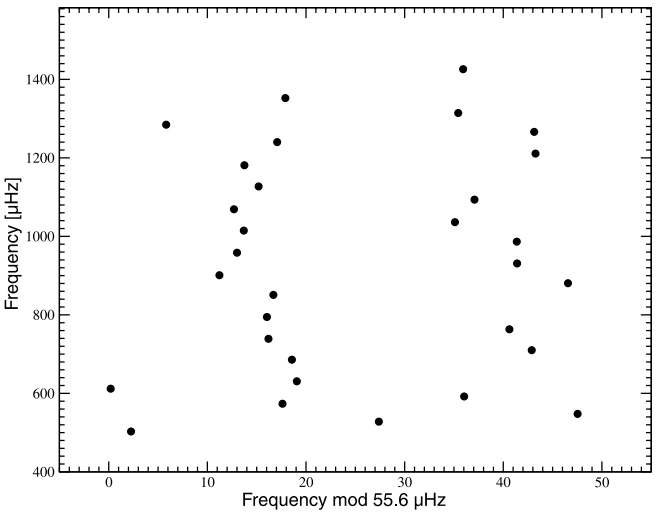

FIG. 11.—Echelle diagram of the *MOST* 2007 Procyon data, where frequencies have been extracted by a technique (see text) that assumes modes have short lifetimes; i.e., they come and go over time. The frequency uncertainty of ± 2.3 μHz is set by the 5 day–long bins used to sample the photometric time series in this technique.

which he compares the Robinson et al. (2003) to the work of Stein & Nordlund (1998) and to the CO5BOLD (Conservative Code for the Computation of Compressible Convection in a Box of L Dimensions with $l = 2$, 3; B. Freytag et al. 2004[4]), respectively. Away from the domain boundaries, where different simplifying assumptions are made, the agreement is satisfactory.

[4] See http://www.astro.uu.se/~bf/co5bold/co5bold.html.

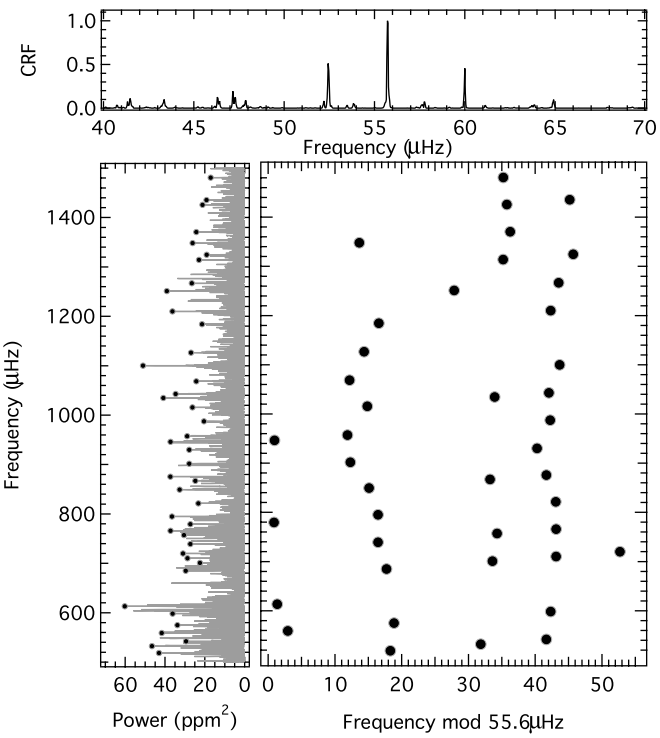

FIG. 12.—*Top*: Comb response function (CFR) of the *MOST* 2007 Procyon power spectrum in the frequency range 500–1500 μHz. (The CRF is scaled in arbitrary units.) *Bottom left*: Procyon power spectrum with comb-filtered peaks indicated by dots. *Bottom right*: Echelle diagram of the extracted peak frequencies.

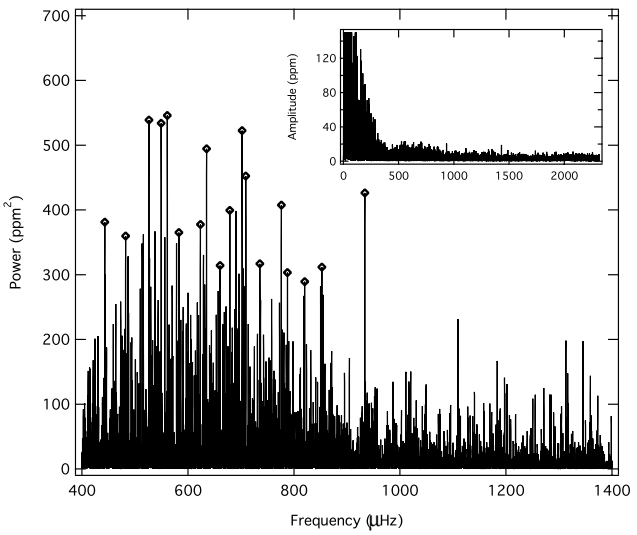

FIG. 13.—Power spectrum of simulated granulation noise containing an artificially generated power "hump" around 600 μHz; the full frequency range is shown in the inset. The peaks labeled with diamonds were identified by the comb filtering procedure as described in the text and shown in the comb response in Fig. 14.

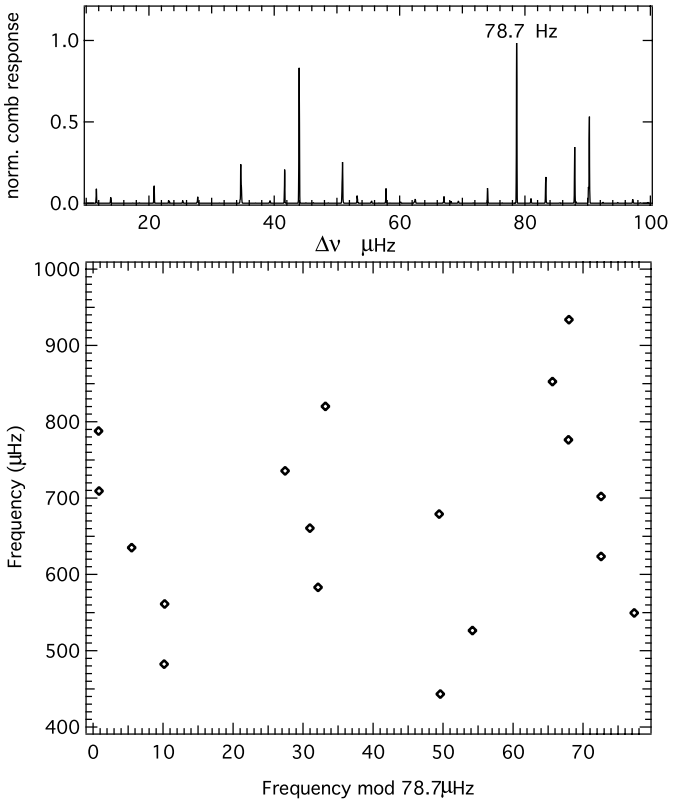

FIG. 14.—Comb response function (*top*) and echelle diagram of the comb-filtered peaks (*bottom*) extracted from the simulated granulation noise shown in Fig. 13.

Although only a small piece of Procyon's convection zone is modeled (the largest box is 29 Mm $\times$ 29 Mm $\times$ 16.3 Mm), the simulation is physically realistic. A current equation of state (OPAL EOS2005; Rogers et al. 1996) and opacities (OPAL2005 for high temperatures; Ferguson et al. [2005] for low temperatures) are used. Both log g and the energy flux are matched to Procyon, as well as the chemical composition. The Yale convection group's results, although tentative, are instructive, demonstrating the clear connection between convection and asteroseismology.

We use power density plots to compare the surface features of the convection simulations to the photometric observations by *MOST*. Figure 15*a* shows power density spectra for the *MOST* 2007 data, along with the *MOST* 2004 and 2005 data and the *WIRE* 2000 photometry (Bruntt et al. 2005). In Figure 15*b* we show the amplitude spectra for *MOST* 2007 and *WIRE* 2000. Figure 15*b* illustrates the low noise achieved by a long uninterrupted time series of precise photometry. Note that the faster readout time for the detector in *WIRE* compared to *MOST* allows for a higher cadence rate and a resulting lower point-to-point noise level, resulting in a lower power density curve (Fig. 15*a*). The power density puts the data sets on the same footing in the sense of time sampling. *MOST* loses the benefit of the long continuous time sampling in this comparison. The smaller dead time for readout between exposures means higher counts for an "exposure" for *WIRE* in the same time interval as a *MOST* exposure. The high-frequency range is where *WIRE* performs best.

We draw attention to the slight hump near 1000 μHz, which corresponds to the expected range of *p*-modes in Procyon, seen in the power density spectra of the *MOST* and *WIRE* data (Fig. 15*a*) and in the amplitude spectrum of the *WIRE* data (Fig. 15*b*). The power hump can have many origins that have little to do with periodic motions on the surface of Procyon. The more pronounced power hump in *WIRE* data, for example, might be at least partially due to the spectral window of the observations. The fact that the strength of the hump dramatically drops after prewhitening low-frequency power from the *WIRE* photometry (Fig. 15*a*, *dashed gray line*) is an indication that the hump is at least partially connected to the spectral window.

In Figure 16 we show a power density plot based on the Yale convection simulation. To obtain this plot we took the run of temperature at optical depth $\tau = 1$ in the convection simulation and converted it to a luminosity variation. Since the simulation only covers several hours of real time we appended together random subsets of random lengths of the simulation to match the *MOST* Procyon 2007 run. Although we repeated this assembly for different random subsets and different random lengths, the resulting power density plots were nearly the same.

The Procyon convection simulation shows a slight hump at 1000 μHz in the power density plot (Fig. 16), similar to that seen in the observations of Procyon (Fig. 15*a*). Although acoustic waves are allowed in the simulation, the duration of the simulation and the box size are too small to support a spectrum of *p*-modes. The hump is relatively broad and shallow and its location in frequency is consistent with the range of granulation lifetimes, in the interval from 10 to 20 minutes.

Because the temperature in the Procyon atmosphere is higher than in the Sun, the superadiabatic layer (SAL) is closer to the surface in Procyon and the top of the granulation penetrates the optically thin layers, giving rise to the phenomenon of "naked granulation" discussed previously in the context of Procyon granulation by Dravins & Nordlund (1990). As a result, we expect the outer atmospheric layers in Procyon to be more sensitive to the granulation signal than in the Sun. At the same time, box modes, which are artifacts forced by the assumed boundary conditions (top and bottom were closed lids) can appear in the simulated power plots. By opening up the top and allowing the simulation to reach its new equilibrium the strongest box eigenmodes were removed and the granulation signal revealed.

As a further test, we have constructed a similar power density curve based on the Yale convection group's simulation of the Sun's convection zone (Fig. 16). The solar simulation data provide additional evidence that the observed bump in the *MOST* and *WIRE*

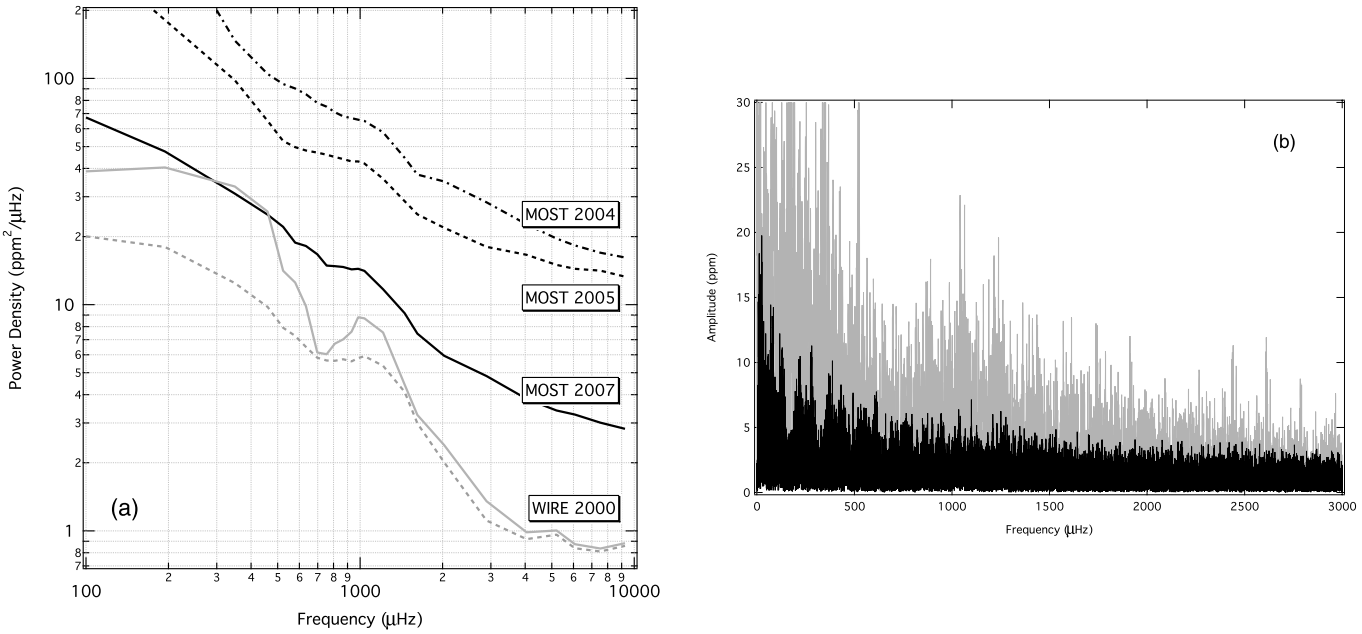

FIG. 15.—(*a*) Power density spectra of *MOST* photometry of Procyon compared to *WIRE* photometry (Bruntt et al. 2005). (*b*) Amplitude spectra comparing photometry for Procyon from *MOST* 2007 (*black curve*), identical to Fig. 3, to *WIRE* 2000 (*gray curve*).

data is due at least in part to granulation. The solar power density plot does not show a hump at 1000 μHz. Rather, it has a small hump in the vicinity of 1500 μHz, which corresponds to the frequency range of solar granulation. Note that the peaks at 2500 and 4000 μHz are known to be due to box modes as the simulation used closed top and bottom boundary conditions. In the case of the Sun, where the granulation has a relatively small effect on the outer atmospheric structure, we expect the signature of the granulation to be weak and barely detectable. The presence of a granulation peak in the solar simulation power density plot thus strongly suggests by analogy that the 1000 μHz hump in Procyon is possibly also associated with granulation.

The convection simulations yield several other results that may be important for understanding Procyon's pulsations. The first result is related to the shallow position of the superadiabatic layer (SAL) in the Procyon atmosphere. We speculate that this may be responsible for the short lifetimes of *p*-modes observed in Procyon. It is plausible to infer that the large radiative losses in the SAL, the region in the convection envelope that contributes mostly to the driving of the *p*-modes, result in more efficient radiative damping and therefore in shorter lifetimes for the *p*-modes in Procyon than in the Sun.

Another possibly important result of the simulation is the remarkable coincidence between the frequency of the granulation signature and the expected frequency range of the Procyon *p*-modes (both peaking at about 1000 μHz). This coincidence does not arise in the Sun where the granulation power peak occurs at 1500 μHz and the *p*-mode power peak occurs at 3000 μHz.

The coincidence in frequency of the granulation and *p*-mode signals in Procyon provides a natural explanation for the hitherto unexplained result that, unlike for the Sun and other Sun-like stars, *p*-mode oscillations have been detected in RV measurements and not in intensity measurements. In RV studies such as the ground-based observations, the *p*-mode signal (m s^{-1}) is several orders of magnitude smaller than the granulation signal (km s^{-1}), and can be readily separated in a Doppler measurement. RV measurements of *p*-modes themselves are unaffected by the granulation lifetime. In RV measurements, so many granules contribute to the exposure that while there is a decrease in the net RV due to the hotter rising component of the granules, there is no net periodic variation. The weaker *p*-modes are coherent across the stellar disk, producing a detectable, superimposed periodic signal. On the other hand, when making intensity observations as in *MOST*, the *p*-mode oscillation frequencies appear in the power spectrum in the same frequency range as the granulation signal. The overlap in Procyon of the *p*-mode frequency peaks with the stochastic

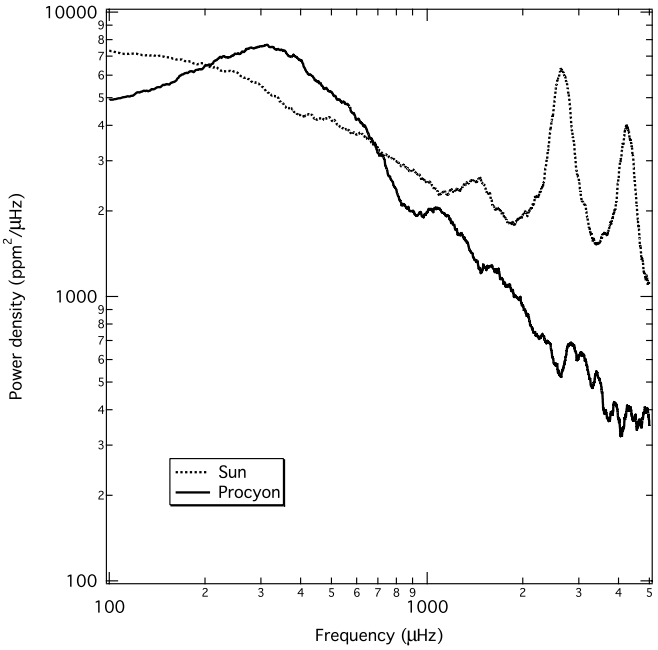

FIG. 16.—Power density spectrum of a hydrodynamical simulation of Procyon's convective envelope, compared to a similar model for the Sun. The shallow hump at 1000 μHz in the Procyon simulation is due to granulation. The shallow hump at 1500 μHz in the solar simulation is also due to granulation. Note, however, that the two sharply peaked humps at 2500 and 4000 μHz in the solar simulation are artifacts of the simulation box.

granulation signal thus make *p*-mode detection in intensity extremely difficult.

The differences in atmospheric structure (its thinness and associated naked granulation) and dynamics (the simulations show an oscillating superadiabatic layer that moves up and down on timescales of between 10 and 30 minutes) between Procyon and the Sun also suggest that it is unlikely that the *p*-mode signal on Procyon will be completely Sun-like.

6. SUMMARY AND CONCLUSIONS

Procyon's thin convection zone is structurally and dynamically distinct from the Sun's, so Procyon represents a laboratory to explore and better understand the interactions of *p*-mode oscillations and granulation in solar-type stars.

The *MOST* 2007 Procyon photometry has the time baseline, sampling and complete coverage (free of significant aliasing due to gaps in the time series), and the precision, to give the best sensitivity to luminosity variations due to *p*-modes and granulation in Procyon. The spectral power density and amplitude spectra of the data show a hump centered near 1000 μHz (unassociated with leakage of power from lower frequencies or instrumental artifacts), which does correspond to the expected location of the peak of *p*-mode power in Procyon. However, this also matches the peak in power associated with granulation as revealed in new numerical simulations of Procyon's convective envelope. This is the first direct observational test of the temporal behavior of these convection models.

Autocorrelation of the Procyon amplitude spectrum (in the predicted *p*-mode range of 500–1500 μHz) does produce a peak near 56 μHz that matches, within the uncertainties, the large frequency spacing $\Delta\nu$ predicted by stellar models of Procyon. However, we are unable to extract individual *p*-mode candidate frequencies that appear as well-defined ridges in an echelle diagram, unless we bias the frequency extraction by assuming short mode lifetimes. The echelle diagrams based on short-lived modes (and hence significant *p*-mode amplitude variations over the course of the *MOST* 2007 Procyon run) do show vertical ridges, each characteristic of modes sharing the same degree *l*. However, the ridges still exhibit scatter about the mean of about ± 5 μHz, which simple stellar models cannot explain. This scatter is consistent with the scatter seen in and among other published echelle diagrams based on ground-based RV observations of Procyon.

The numerical simulations of convection presented in this paper suggest that the shallow depth of the superadiabatic layer (SAL) in Procyon (the region in the convective envelope which is most important in *p*-mode driving) leads to large radiative losses in the SAL and hence more efficient radiative damping. This and the oscillatory up-and-down motion of the SAL with timescales of 10–30 minutes revealed by the simulations are strong culprits to account for short mode lifetimes in Procyon compared to the Sun. Although Procyon cannot be observed by the *COROT* mission (nor will it be a viable target for *Kepler* when its mission begins), we look forward to future observations of Procyon-like objects from *COROT* and *Kepler*, which should permit more detailed tests of the interactions between acoustic oscillations and convection in solar-type stars.

The Natural Sciences and Engineering Research Council of Canada supports the research of D. B. G., J. M. M., A. F. J. M., S. M. R., and G. A. H. W. FQRNT (Québec) also supports A. F. J. M., and R. K. is supported by the Canadian Space Agency. T. K., M. G., and W. W. W. are supported by the Austrian Research Promotion Agency (FFG), and the Austrian Science Fund (FWF P17580). P. D. and F. J. R. are supported by grant NASA/ATP NAG5-13299 with additional support to F. J. R. from NASA EOS/IDS.

REFERENCES

Allende Prieto, C., Asplund, M., García López, R. J., & Lambert, D. L. 2002, ApJ, 567, 544
Baudin, F., Appourchaux, T., Boumier, P., Kuschnig, R., Leibacher, J. W., & Matthews, J. M. 2008, A&A, 478, 461
Bedding, T. R., et al. 2005, A&A, 432, L43
Brown, T. M., Gilliland, R. L., Noyes, R. W., & Ramsey, L. W. 1991, ApJ, 368, 599
Bruntt, H., Kjeldsen, H., Buzasi, D. L., & Bedding, T. R. 2005, ApJ, 633, 440
Chaboyer, B., Demarque, P., & Guenther, D. B. 1999, ApJ, 525, L41
Chaplin, W. J., Houdek, G., Appourchaux, T., Elsworth, Y., New, R., & Toutain, T. 2008, A&A, 485, 813
Chaplin, W. J., et al. 1997, MNRAS, 287, 51
Christensen-Dalsgaard, J., & Frandsen, S. 1983, Sol. Phys., 82, 469
Dravins, D., & Nordlund, A. 1990, A&A, 228, 203
Eggenberger, P., Carrier, F., Bouchy, F., & Blecha, A. 2004, A&A, 422, 247
Ferguson, J. W., Alexander, D. R., Allard, F., Barman, T., Bodnarik, J. G., Hauschildt, P. H., Heffner-Wong, A., & Tamanai, A. 2005, ApJ, 623, 585
Gatewood, G., & Han, I. 2006, AJ, 131, 1015
Girard, T. M., et al. 1996, BAAS, 28, 919
———. 2000, AJ, 119, 2428
Guenther, D. B., & Demarque, P. 1993, ApJ, 405, 298
Guenther, D. B., et al. 2007, Commun. Asteroseis., 151, 5
Hekker, S., et al. 2007, preprint (arXiv:0710.3772v1)
Houdek, G., Balmforth, N. J., Christensen-Dalsgaard, J., & Gough, D. O. 1999, A&A, 351, 582
Irwin, A. W., Fletcher, J. M., Yang, Stephenson L. S., Walker, G. A. H., & Goodenough, C. 1992, PASP, 104, 489
Kjeldsen, H., & Bedding, T. R. 1995, A&A, 293, 87
Kupka, F. 2005, in Proc. Interdisciplinary Aspects of Turbulence, ed. F. Kupka & W. Hillenbrandt (Garching: MPI), 141
———. 2008, in Interdisciplinary Aspects of Turbulence, ed. W. Hillerbrandt & F. Kupka (Berlin: Springer), in press
Leccia, S., Kjeldsen, H., Bonanno, A., Claudi, R. U., Ventura, R., & Paternó, L. 2007, A&A, 464, 1059
Marchenko, S. V. 2008, A&A, 479, 845
Martic, M., Lebrun, J.-C., Appourchaux, T., & Korzennik, S. G. 2004, A&A, 418, 295
Martic, M., et al. 1999, A&A, 351, 993
Matthews, J. M., Kuschnig, R., Guenther, D. B., Walker, G. A. H., Moffat, A. F. J., Rucinski, S. M., Sasselov, D., & Weiss, W. W. 2004, Nature, 430, 51
Provost, J., Berthomiew, G., Martic, M., & Morel, P. 2006, A&A, 460, 759
Reegen, P. 2007, A&A, 467, 1353
Reegen, P., et al. 2006, MNRAS, 367, 1417
Régulo, C., & Cortés, T. 2005, A&A, 444, L5
Robinson, F., & Demarque, P. 2007, in Proc. IAU Symp. 239, Convection in Astrophysics, ed. F. Kupka, I. Roxburgh, & K. Chan (Cambridge: Cambridge Univ. Press), 358
Robinson, F. J., Demarque, P., Guenther, D. B., Kim, Y.-C., & Chan, K. L. 2005, MNRAS, 362, 1031
Robinson, F. J., Demarque, P., Li, L. H., Sofia, S., Kim, Y.-C., Chan, K. L., & Guenther, D. B. 2003, MNRAS, 340, 923
Rogers, F. J., Swenson, F. J., & Iglesias, C. A. 1996, ApJ, 456, 902
Schaefer, G., et al. 2006, BAAS, 38, 1104
Stein, R. F., & Nordlund, A. 1998, ApJ, 499, 914
Walker, G. A. H., et al. 2003, PASP, 115, 1023